Light-Induced Charge Separation and Redox Chemistry at the Surface of TiO_2/Host−Guest Hybrid Nanoparticles

Nada M. Dimitrijevic,* Tijana Rajh, Zoran V. Saponjic, Linda de la Garza, and David M. Tiede

Chemistry Division, Argonne National Laboratory, 9700 S. Cass Avenue, Argonne, Illinois 60439

Received: March 3, 2004; In Final Form: April 9, 2004

The photoinduced charge transfer between guest molecules and hybrid TiO_2/cyclodextrin nanoparticles was studied using low-temperature EPR and cyclic voltammetry. The photoexcitation of TiO_2 at 4.6 K yields to the localization of valence band holes at carboxyl groups of surface-conjugated cyclodextrin and conduction band electrons at lattice Ti atoms. The presence of 1-adamantanol in the cyclodextrin cavity does not affect charge separation and trapping because of its unfavorable oxidation potential. However, when ferrocenemethanol ($E_{ox} = 0.52$ V vs NHE) was used as the guest molecule the formation of ferrocenium cation was observed, revealing electron transfer from guest molecules to TiO_2 nanoparticles. This results in dissociation of the host−guest assembly because of repulsion of the charged ion from the hydrophobic cavity of cyclodextrin into the bulk of the aqueous solution and consequently leads to efficient charge separation and redox chemistry.

Introduction

Successful photochemical energy conversion and subsequent chemical reactions require extended separation of photogenerated charges. In semiconductor nanoparticles, the separation between photogenerated electrons and holes is limited by the particle size and results in fast recombination of charge carriers. Our approach to achieving enlarged separation distances is to remove one of the photogenerated charges, such as valence band holes, by coupling the electron-donating agents capable of shuttling a charge to a mobile redox couple to the surface of TiO_2 nanoparticles ($d = 45$ Å). We have chosen β-cyclodextrin (β-CD) both as an electron-donating and molecular-recognizing agent. β-CD comprises seven α-1,4 linked glucopyranose units organized in a toruslike macroring structure and possesses the hydrophobic cavity dimensions ~7 Å capable for inclusion of water insoluble compounds.[1] The ability of cyclodextrins to engage in molecular[2] and chiral[3] recognition through host−guest inclusion complexes attracts renewed interest in the construction of various supramolecular architectures.[4] Tailored assembly of α-CD on gold substrate was recently reported for host−guest complexation with azobenzene and photochemically controlled patterning of nanotubes.[5] In general, cyclodextrins, when physisorbed/chemisorbed on semiconductors, increase the stability of particles and enhance the yield of photoinduced charge-transfer reactions.[6] When linked to the semiconductor nanoparticles, β-CDs could act as multiple charge relays between photogenerated holes and guest molecules. Thus, because of the selectivity of the β-CD-host cavity (hydrophobic, dimensional, and structural discrimination), the interfacial molecular recognition could be combined with interfacial charge transfer on semiconductor particles. By selective linking of β-CD to TiO_2 nanoparticles, we expect to improve both selective charge separation and consecutive selective redox chemistry of the guest molecules. We linked carboxyethyl β-cyclodextrin (CE-β-CD) to TiO_2 particles to obtain tailored semiconductor−receptor configuration. β-cyclodextrin was linked to the surface Ti atoms of TiO_2 nanoparticles via carboxyl groups attached to the cyclodextrin ring. In our previous work,[7] we have demonstrated that β-CD bound to TiO_2 by carboxyl groups or via a dopamine bridge efficiently promotes charge separation of photogenerated carriers. As a probe of the efficiency of extended charge separation of photogenerated carriers, we used the ability of electrons to reduce silver nitrate on the surface of particles. In this paper, we report light-induced charge separation and interfacial electron transfer that extends from cyclodextrin-modified TiO_2 to the guest molecule residing in the CD cavity. Low-temperature electron paramagnetic resonance (EPR) was employed to examine the initial separation of photogenerated charges. Electrochemical measurements on thin film TiO_2 electrodes were performed to understand the mechanism of charge transfer between CD-modified TiO_2 and guest molecules. Additionally, synchrotron-based X-ray scattering was employed to elucidate formation and dissociation of the inclusion complex between cyclodextrin and ferrocenemethanol.

Experimental Section

Chemicals. All the reagents were analytical grade and used as received, without further purification. CE-β-CD having 3.2 ± 0.4 carboxyl groups per molecule was purchased from Fluka. Milli-Q deionized water (resistivity 18.2 MΩ cm^{-1}) was used for synthesis.

Nanocrystal Synthesis and Modification. The preparation and characterization of TiO_2 nanoparticles is described elsewhere[8] and only outlined herein. The seeds of colloidal TiO_2 were prepared by dropwise addition of titanium(IV) chloride to cooled water using an apparatus developed for controlling the temperature and rate of mixing reaction components.[9,10] Slow growth of the particles was achieved by dialysis at 4 °C against water until the pH of the solution reached pH 3.5, when the growth of crystalline particle TiO_2 was complete. The titania particles were 42.8 ± 3.5 Å in diameter. The surface modification of nanoparticles was obtained by mixing carboxyethyl-β-cyclodextrin with TiO_2 colloidal particles in 20:1 (molecule to particle) ratio. The CE-β-CD binds to the surface of TiO_2

* Address correspondence to this author. E-mail: dimitrijevic@anl.gov.

10.1021/jp049028d CCC: $27.50
Published on Web 05/27/2004

particles through the chelating complex of carboxyl groups with surface Ti ions, as was determined from diffuse reflectance FTIR spectroscopy of powdered samples and described previously.[7]

The TiO_2 electrodes were made by repeated dipping of an ITO glass slide into a concentrated solution (0.3 M) of titania nanoparticles and then heating at 140 °C. The surface of the electrode was ~1.0 cm^2.

Apparatus. X-band EPR experiments were conducted on a Bruker ESP300E spectrometer equipped with a Varian cavity and a variable-temperature cryostat (Air Products) cooled to liquid helium temperature. The microwave frequency was determined after each measurement using a Hewlett-Packard 5352B frequency counter. The g factors were calibrated for homogeneity and accuracy by comparison to a coal standard, $g = 2.00285 \pm 0.00005$. Samples were excited using a 300-W Xe lamp (ILC) with a 360-nm band-pass filter. The filter was used to avoid possible excitation of ferrocene and was applied for all samples.

Cyclic voltametry measurements were performed with three component systems containing TiO_2 as working, Pt as a counter, and Ag/AgCl as a reference electrode, using a BAS-100B/W (Bioanalytical Systems) workstation with a single compartment quartz cell.

Synchrotron-based small and wide-angle X-ray scattering (SAXS/WAXS) data were collected at the 12-BM beamline of the Advance Photon Source of Argonne National Laboratory using a 18 keV X-ray beam. Other operating conditions were similar to those described previously.[11] Atomic pair distribution function (PDF) analysis was determined from experimental scattering data using the program GNOM[12,13] and compared to PDF calculated from coordinate models of the β-CD and β-CD/ferrocene complexes using procedures described previously.[14]

Results and Discussion

EPR of Photogenerated Charges. The photoexcitation of TiO_2 with energies greater than its band gap (3.2 eV) results in the formation of conduction band electrons and valence band holes.

$$TiO_2 \xrightarrow{h\nu} (e_{CB}^- + h_{VB}^+)TiO_2 \qquad (1)$$

Photogenerated carriers can be trapped in the interior of TiO_2 particles or migrate to the surface where they localize at surface-trapping sites. EPR spectroscopy has been widely used to examine paramagnetic species on TiO_2 surfaces.[9,15−20] Before surface modification, the EPR spectrum obtained upon illumination of degassed aqueous bare TiO_2 is composed of two sets of signals: (i) holes trapped at the surface OH groups as $(TiO_2)_n$-$Ti^{IV}O^{\bullet}$, where $(TiO_2)_n$ represents bulk materials, characterized by g-factor values >2.0,[16−18] and (ii) electrons trapped in the interior or at the surface of particles with $g < 2.0$ (Figure 1a).[9,19,20] The oxygen radical signals, which are characteristic for trapped holes at TiO_2, exhibit anisotropic g-tensors with $g_z = 2.007$, $g_y = 2.014$, and $g_x = 2.024$.[17,18] The signals associated with trapped electrons are those due to lattice $Ti(III)_{latt}$ (sharp signal at $g_\perp = 1.988$) and surface $Ti(III)_{surf}$ centers (broad signal with $g_\perp = 1.924$).[15,16,19,20] As indicated in Figure 1a, the interior lattice Ti(III) exhibits parallel signals with $g_{||}^1 = 1.961$ and $g_{||}^2 = 1.958$. The splitting of the parallel component indicates that there are two paramagnetic Ti(III) species contributing to the overall signal. The higher field parallel component was previously assigned to electrons localized on interstitial Ti atoms (shallow defects),[17,18,21] while the narrow component at $g_{||}^1 = 1.961$ was associated with a signal that is motionally narrowed

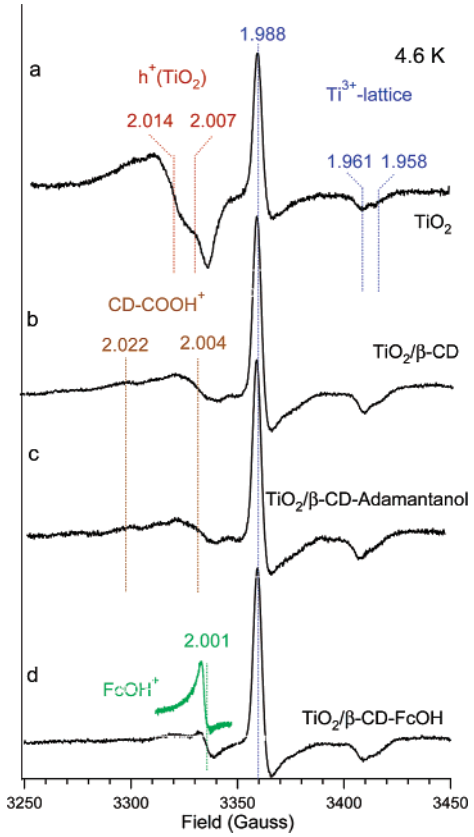

Figure 1. X-band EPR spectra obtained at 4.6 K after illumination (with 360-nm band-pass filter) of (a) unmodified TiO_2 particles, (b) carboxyethyl-β-cyclodextrin modified TiO_2 particles, TiO_2/CE-β-CD, (c) TiO_2/CE-β-CD with addition of 1-adamantanol in 1:2 molar ratio to cyclodextrin, and (d) TiO_2/CE-β-CD with addition of ferrocenemethanol in 1:2 molar ratio to cyclodextrin.

by an electron hopping from one center to another (delocalized electrons).[22] A similar signal has been observed from partially reduced rutile TiO_2 and attributed to an electron loosely bound to an interstitial titanium ion or a completely delocalized electron.[23]

When particles were modified with CE-β-CD, the characteristic oxygen radical signal (trapped holes on the surface of TiO_2) in the EPR spectrum obtained after illumination of titania disappears, and a new feature composed mainly of g-factors of 2.004 and 2.022 appears (Figure 1b). In our previous study of methyl cysteine (and its derivatives) bound through carboxyl groups to TiO_2, we have demonstrated that hole localization onto carboxyl groups results in oxygen-centered radicals having EPR spectrum with the same g-tensors of 2.004 and 2.022.[9] Thus, we assign the signals with $g > 2$ in Figure 1b to oxygen-centered radicals on carboxyl groups. The IR spectra of CE-β-CD attached to TiO_2 particles further support assignment of EPR spectra to oxygen-centered radicals. Specifically, IR spectra have shown that oxygens from carboxyl groups are bound to the surface Ti atoms of TiO_2 particles.[7] Thus, carboxyl groups act as the initial trapping sites for photogenerated holes. Strong oxidizing radicals, such as $^{\bullet}OH$ and $SO_4^{-\bullet}$, react nonselectively with cyclodextrins that do not have carboxyl groups.[24,25] It has been shown by EPR (room-temperature measurements) that the reaction involves H abstraction from CD toruslike ring. The resulting carbon-centered radicals are positioned both inside and outside of the CD cavity. For β-cyclodextrin, the predominant position of carbon-centered radicals is inside the cavity (C3 and C5 radicals), having a g-factor of 2.0032, but different hyperfine splitting.[24] The attachment of carboxyl groups onto β-CD can

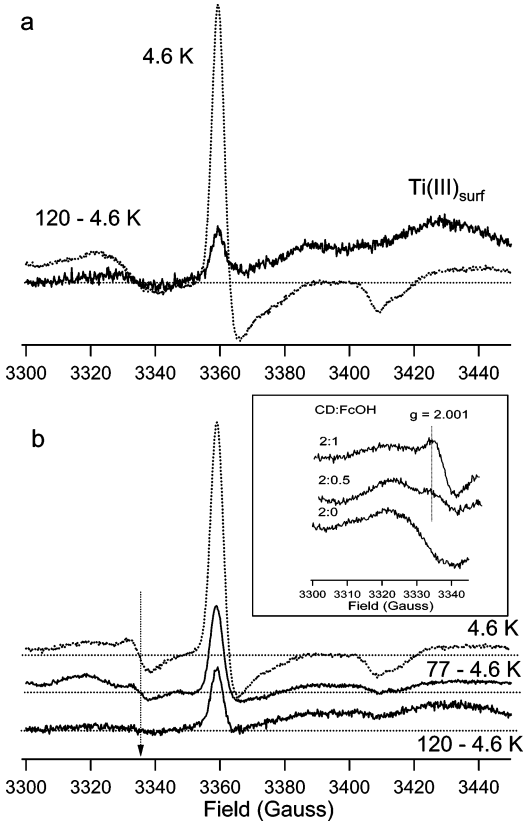

Figure 2. X-band EPR spectra measured at 4.6 K after illumination (with 360-nm band-pass filter) at elevated temperatures of (a) carboxyethyl-β-cyclodextrin modified TiO_2 particles, TiO_2/CE-β-CD, and (b) TiO_2/CE-β-CD with addition of ferrocenemethanol in 1:2 molar ratio to cyclodextrin. The dotted lines represent EPR signals of samples illuminated at liquid-helium temperature. Inset: X-band EPR spectra measured at 4.6 K after illumination of TiO_2/CE-β-CD before and after addition of ferrocenemethanol in 1:2 and 0.5:2 molar ratio to cyclodextrin.

facilitate oxidation by providing a deeper trapping site that attracts holes in primary events. In our experiments, the detection of carbon-centered radicals on CD torus cannot be resolved from the carboxyl-centered radicals because of the line broadening of EPR signals at low temperatures. However, the existence of carbon-centered radicals could not be ruled out, as they can contribute to the overall EPR spectrum, as well as to the overall charge-transfer processes. As can be seen from Figure 1b, the shape of the signals that correspond to the trapped electrons was not changed. However, we detected more intense $Ti(III)_{latt}$ signals compared to bare TiO_2 as a consequence of enhanced charge separation that results in a larger number of electron−hole pairs.

Photoexcitation of TiO_2/CE-β-CD hybrid particles at 120 K results in the decrease of the signal for lattice-trapped $Ti(III)_{latt}$ electrons and the increase of the signal corresponding to the surface-trapped $Ti(III)_{surf}$ electrons, Figure 2a. By increasing the temperature, a transfer of electrons from the interior of the particle to the surface-trapping sites occurs.[9] For 45 Å particles there is ~400 surface Ti atoms per particle,[20] thus with the ratio of CD to particles as low as 20:1, there is more than 80% of free unmodified surface Ti sites capable of trapping electrons.

The EPR spectrum of photoinduced charges in a hybrid TiO_2/CE-β-CD particle was not affected by the presence of 1-adamantanol, Figure 1c. Adamantane molecules (and derivatives) are guests of choice because of their tight inclusion into the cavity of β-CDs.[26,27] However, the very high oxidation potential of adamantane, $E_{ox} = 2.96$ V versus NHE,[28] does not allow transfer of even valence band holes ($E_{VB} = 2.9$ V at pH 3.5) to occur. Consequently, inclusion of adamantanol into hybrid TiO_2/CE-β-CD particles does not charge the charge transfer cascade, and the EPR spectrum shows only the presence of carboxyl-centered radicals. When ferrocenemethanol (FcOH) was used as a guest molecule, the formation of ferrocenium ion, $FcOH^+$, was observed revealing electron transfer between TiO_2 nanoparticles and guest molecules (Figure 1d). The relative intensity of the signal depends on the ratio of CE-β-CD:FcOH (Figure 2a, inset). The FcOH incorporated into the CD cavity is able to seize holes from hybrid TiO_2/CD particles. Thus, CD on the surface of TiO_2 acts as a relay in the charge-transfer process that extends charge separation and promotes redox chemistry.

The redox potential of FcOH inside the cyclodextrin cavity shifts ~100 mV more positive compared to the molecule in aqueous solution, the value $E_{ox} = 0.52$ V versus NHE was determined from cyclic voltammetry measurements. This potential is more negative than the potential of valence band holes of TiO_2 or carboxyl-centered radicals of cyclodextrin, thus promoting enhanced electron transfer. For comparison, Figure 2 also contains an EPR spectrum of blue-colored ferrocenium cation synthesized from ferrocenemethanol according to the literature procedure.[29] The axial-type EPR signal with $g_\perp = 2.001$ is typical of a ferrocenium cation in which the electron is removed from the iron center in a ferrocenium complex.[30−32] This species is characterized by fast spin−lattice relaxation, detectable only at liquid-helium temperature. Thus, samples were illuminated at elevated temperatures and EPR spectra measured in the dark upon freezing to 4.6 K. The increase in the temperature yields to the loss of both the ferrocenium cation and lattice-trapped electron signals, Figure 2b. This suggests the recombination reaction between TiO_2 trapped electrons and $FcOH^+$; the ferrocenium cation is a very strong oxidizing agent which can be easily reduced to a neutral ferrocene molecule with TiO_2 surface-trapped electrons. On the other hand, $FcOH^+$ as the charged species can diffuse from the cyclodextrin cavity into the bulk of the solution at room temperature, thus escaping from the surface of TiO_2 particles and charge recombination (Scheme 1). The association constant for complexation of a ferrocenium cation with cyclodextrins is an order of magnitude lower[33] as compared to the neutral FcOH ($K_{FcOH/CE-\beta-CD} = 2.1 \times 10^3$ M^{-1}, Supplement 1). To further elucidate the fate of $FcOH^+$, we have performed room-temperature synchrotron-based X-ray scattering measurements of aqueous host−guest complexes and voltammetric measurements on thin film TiO_2 electrodes.

SAXS/WAXS Measurements. To directly monitor and characterize dissociation of a host−guest complex upon oxidation of FcOH incorporated into a CE-β-CD cavity, we used a synchrotron-based wide-angle X-ray scattering (WAXS) technique[34,35] combined with atomic pair distribution function (PDF) analysis.[12,13] The technique enables in-situ structural characterization of noncrystalline materials, which can achieve atomic-scale resolution for small molecular compounds.[36−40] WAXS data were collected with 2.1 Å spatial resolution through measurements across the range of momentum transfer 0.05 $Å^{-1} < q < 3$ $Å^{-1}$, where $q = (4\pi/\lambda)\sin\theta$, λ is the X-ray wavelength, and 2θ is the scattering angle, using an 18 keV X-ray beam. The structure of a model β-CD-ferrocene complex is shown in Figure 3a, and the corresponding electron density weighted PDF calculated with respect to the solvent water is shown for the β-CD host (blue line) and β-CD-ferrocene (red line) model structures in Figure 3b. The electron density pair correlations calculated for the β-CD host show characteristic features of a

SCHEME 1 . Schematic Presentation of Photogenerated Charge Transfer in Hybrid TiO_2/CD Particles (a) in the Absence and (b) in the Presence of FcOH[a]

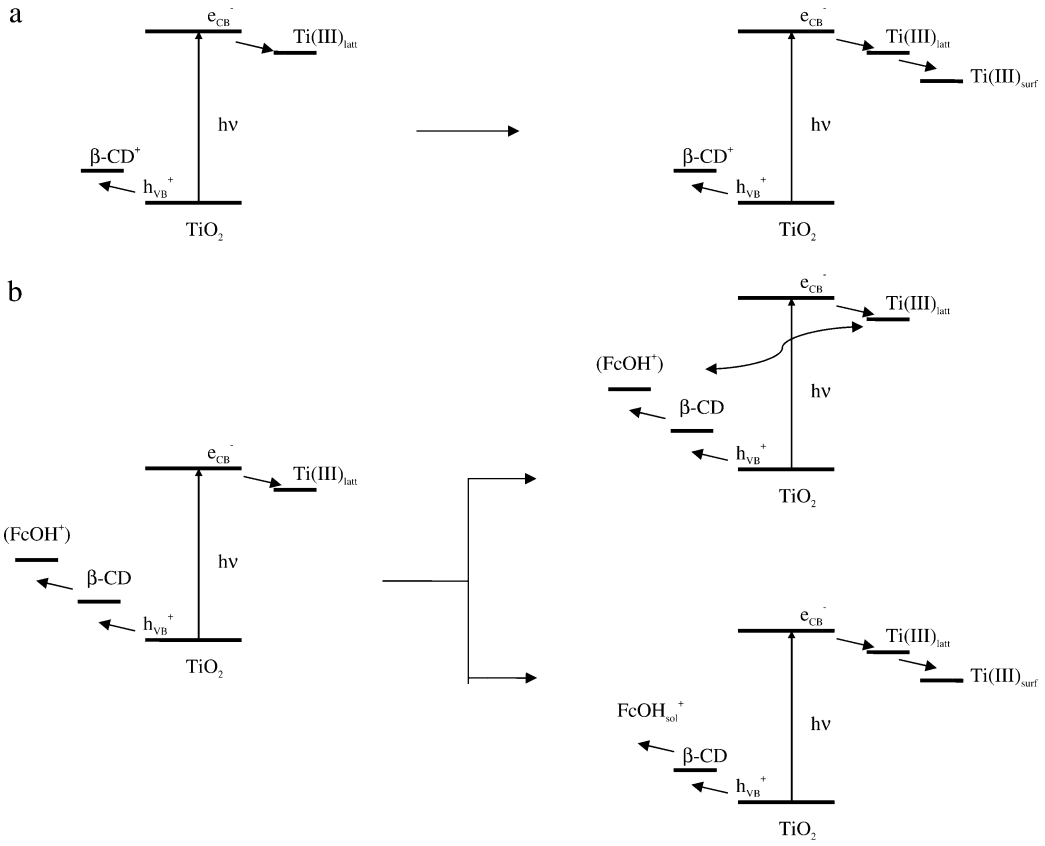

[a]The parenthesis represent ferrocenemethanol in the inclusion complex.

conical ring structure, having a peak at 10.8 Å and trough at 13.3 Å that arise from variations in the electron density weighted pair correlations across the conical ring. Insertion of a ferrocene molecule into the CD cavity is seen to introduce a new set of pair correlations centered at 6.1 Å that correspond to radial pair correlations between ferrocene and the cyclodextrin ring.

PDF determined for the CE-β-CD host and CE-β-CD-FcOH and CE-β-CD-$FcOH^+$ host−guest complexes are shown in Figure 3c. Experimental scattering patterns and fits of the Fourier transform PDF to experimental data are shown in the supplementary data. Experimentally determined PDF for the CE-β-CD host (Figure 3c, blue line) shows the characteristic features of the conical ring structure, having a principle pair correlation peak at 10.8 Å and a trough at 13.3 Å comparable to the model structure. The PDF determined from the 10 mM CE-β-CD in aqueous solution in the presence of FcOH (Figure 3c, red line), shows the appearance of a new peak at 6.2 Å arising from the ferrocene guest−host pair correlations, demonstrating the formation of a 1:1 inclusion complex. The changes in the scattering pattern and presence of the 6.2 Å PDF peak directly depend on the concentration of FcOH (from 5 to 10 mM) confirming assembly of a host−guest complex (Supplement 2). The addition of a low concentration of the relatively mild oxidizing agent H_2O_2 into a solution of FcOH/CE-β-CD results in partial formation of $FcOH^+$ which can be observed by the change in color from yellow to green (greenish solution is composed of a mixture of neutral and oxidized ferrocene). The partial formation of $FcOH^+$ shifts the scattering pattern of the FcOH/CE-β-CD mixture toward that of the CE-β-CD alone (Supplement 2). The corresponding PDF in the presence of the partially oxidized FcOH (green line in Figure 3c) shows that the partial oxidation reduces the occupancy of the charged $FcOH^+$ in the hydrophobic CE-β-CD host cavity. This demonstrates the dissociation of the charged molecule $FcOH^+$ from the hydrophobic cavity. Unfortunately, we could not study assembly and dissociation of the host−guest complex on the surface of TiO_2 by the WAXS technique because of strong interference of a diffraction pattern from crystalline particles in the q-range 0.9−3 $Å^{-1}$.

Cyclic Voltammetry on Thin Film TiO_2 Electrodes. We used cyclic voltammetry (CV) measurements to investigate the host−guest phenomena on thin film TiO_2 electrodes. The voltammetric properties of FcOH are expected to respond to the complexation of molecules by interfacial CD. Additionally, following properties of FcOH in the inclusion complex after illuminating the TiO_2 electrode would help establish the mechanism of redox reactions in the hybrid TiO_2/CD particulate system. We used the same thin film TiO_2 electrode in all measurements (changing solutions), thus avoiding differences in thickness and crystallinity of the film and possible defects on the surface which can affect CV measurements.[41] We have examined CVs of FcOH in three different systems: free in aqueous solution, incorporated in β-cyclodextrin that does not have carboxylic groups, and upon addition of carboxyethyl-β-cyclodextrin. The cyclic voltammograms of these systems are presented in Figure 4. As can be seen from Figure 4a, the reversible processes occur at the TiO_2 electrode surface in the free FcOH and FcOH incorporated into the β-CD cavity. The shift of both oxidation and reduction maxima to more positive values in the presence of β-CD clearly indicates that FcOH is forming an inclusion complex with cyclodextrin.[42] When carboxyethyl-β-cyclodextrin was used in the presence of FcOH, the cyclic voltammogram changes in shape and intensity (Figure 4b). The lower current intensity and the lack of distinguished

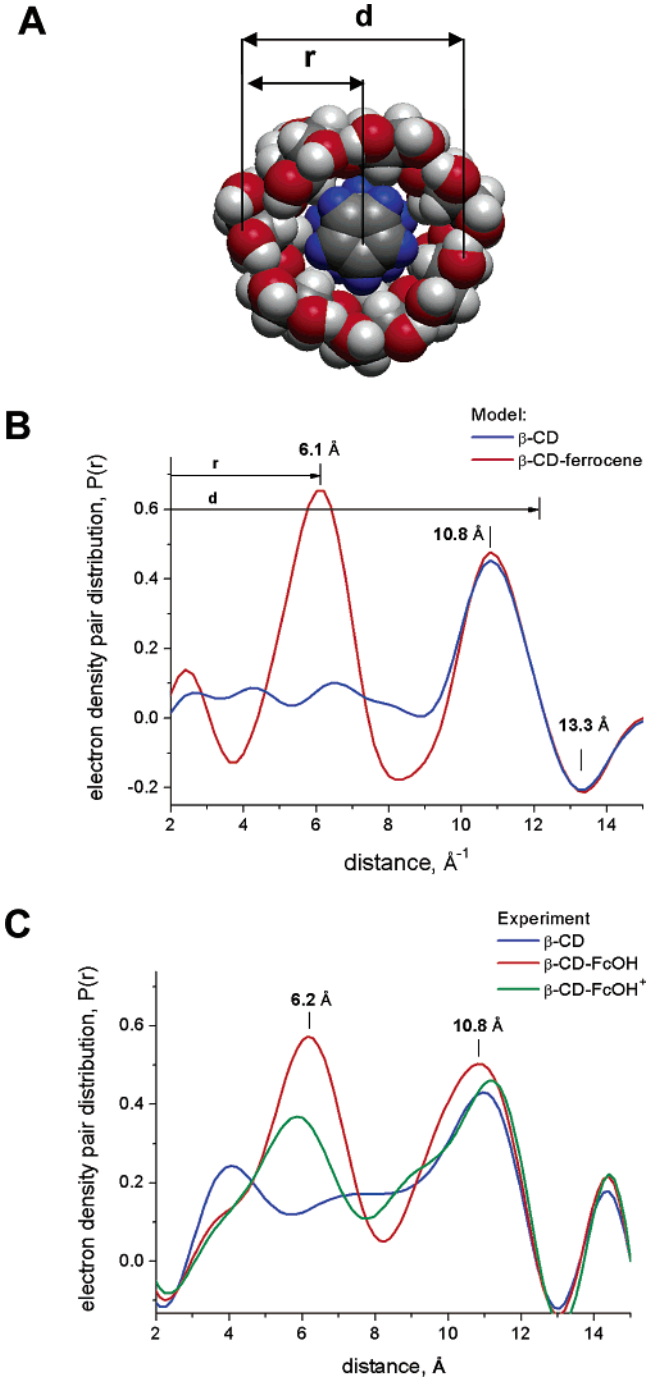

Figure 3. (a) The structure of a model β-CD-ferrocene complex, and (b) corresponding electron density weighted pair distribution functions, PDF, calculated with respect to the solvent water for the β-CD host (blue line) and β-CD-ferrocene complex (red line) model structures; (c) PDF determined from the experimental scattering patterns of the aqueous solution of CE-β-CD (blue line), CE-β-CD in the presence of FcOH (red line) and upon partial oxidation of FcOH (green line).

peaks are results of anchoring cyclodextrins on the surface of the electrode via carboxyl groups. The conjugation of cyclodextrin to the surface of the TiO_2 electrode suppresses reversible oxidation and reduction of FcOH. Similar suppression of well-defined peaks of ferrocene on a CD-thiol conjugated gold electrode was recently reported.[43] The slightly more intense oxidation wave indicates confinement of FcOH at the electrode surface because of its incorporation into the CD cavity and at the same time points to the hydrophobic/hydrophilic repulsion of ferrocenium cation from the surface of the electrode, making detection of the $FcOH^+$ ion more difficult. Nevertheless, after

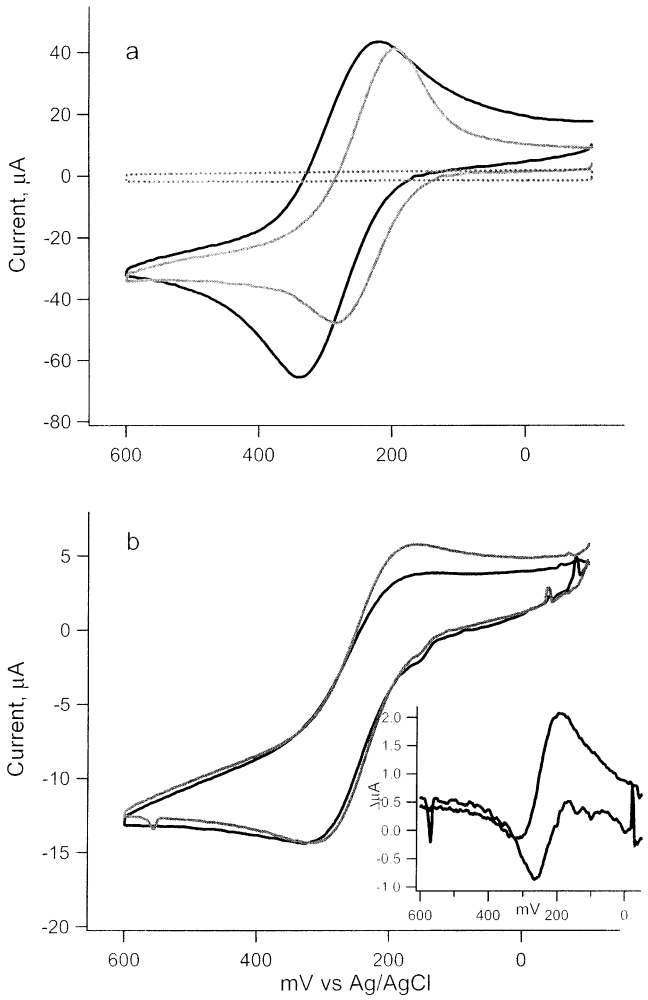

Figure 4. Cyclic voltammograms of (a) 1 mM FcOH in the absence (gray line) and in the presence (black line) of 2 mM β-CD, dotted line: aqueous electrolyte solution; (b) 1 mM FcOH in the presence of 2 mM CE-β-CD before (black line) and after photoexcitation of TiO_2 measured in the dark (gray line). All measurements were performed on an electrode composed of thin film TiO_2 deposited on ITO glass in aqueous solution containing 50 mM NaCl. Scan rate 50 mV/s. Inset: Difference between voltammograms obtained after and before illumination.

photoexcitation of TiO_2, an increase in the intensity of the reduction peak current is observed (gray line in Figure 4b), as a result of formation of $FcOH^+$ due to the reaction of FcOH with photogenerated holes. The generated $FcOH^+$ cation dissociates from CD and is detected in the voltammogram at the potential of the reduction wave that corresponds to free $FcOH^+$ (see inset of Figure 4). During the illumination of an electrode, the rest potential of the system shifts to negative values from its original position, being more negative as the time of exposure to UV light increases. The negative shift arises from the shift in the flat band potential of TiO_2 as photogenerated electrons fill its conduction band, while holes react with molecules at the surface. These photoelectrochemical experiments confirm both charge transfer between photogenerated holes in TiO_2 and FcOH and subsequent dissociation of the inclusion complex.

In summary, we have conducted proof-of-concept experiments which combine molecular recognition by cyclodextrin with selective photoinduced charge-transfer reactions on the surface of TiO_2 hybrid nanoparticles. The results have shown successful selective oxidation of ferrocenemethanol included in the hydrophobic cavity of a cyclodextrin molecule, followed with dissociation of an inclusion complex. The hybrid TiO_2/

host−guest nanoparticles and corresponding photoinduced redox chemistry present promising pathways for molecular machines.

Acknowledgment. Work was performed under the auspices of the Office of Basic Energy Sciences, Division of Chemical Sciences, US-DOE under contract number W-31-109-Eng-38. Critical, expert assistance of the Advanced Photon Source BESSRC-CAT staff for the synchrotron experiments is gratefully acknowledged.

Supporting Information Available: Titration spectra of ferrocenemethanol and wide-angle X-ray scattering of solutions. This material is available free of charge via the Internet at http://pubs.acs.org.

References and Notes

(1) Szejtli, J. *Chem. Rev.* **1998**, *98*, 1743.
(2) Harada, A. Cyclodextrins. In *Large Ring Molecules*; Semlyn, J. A., Ed.; Wiley: Chichester, U.K., 1996.
(3) Kano, K.; Hasegawa, H. *J. Am. Chem. Soc.* **2001**, *123*, 10616.
(4) Harada, A. *Acc. Chem. Res.* **2001**, *34*, 456.
(5) Banerjee, I. A.; Yu, L.; Matsui, H. *J. Am. Chem. Soc.* **2003**, *125*, 9542.
(6) (a) Willner, I.; Eichen, Y. *J. Am. Chem. Soc.* **1987**, *109*, 6862. (b) Willner, I.; Eichen, Y.; Frank, A. J. *J. Am. Chem. Soc.* **1989**, *111*, 1884.
(7) Dimitrijevic, N. M.; Saponjic, Z. V.; Bartels, D. M.; Thurnauer, M. C.; Tiede, D. M.; Rajh, T. *J. Phys. Chem. B* **2003**, *107*, 7368.
(8) Rajh, T.; Tiede, D. M.; Thurnauer, M. C. *J. Noncryst. Solids* **1996**, *207*, 815.
(9) Rajh, T.; Ostafin, A. E.; Micic, O. I.; Tiede, D. M.; Thurnauer, M. C. *J. Phys. Chem.* **1996**, *100*, 4538.
(10) Thurnauer, M. C.; Rajh, T.; Tiede, D. M. *Acta Chem. Scand.* **1997**, *51*, 610.
(11) Tiede, D. M.; Zhang, R.; Seifert, S. *Biochem.* **2002**, *41*, 6605.
(12) Svergun, D.; Barberato, C.; Koch, M. H. *J. Appl. Cryst.* **1995**, *28*, 768.
(13) Svergun, D. I. *J. Appl. Cryst.* **1992**, *25*, 495.
(14) Zhang, R.; Seifert, S.; Thiyagarajan, P.; Tiede, D. M. *J. Appl. Cryst.* **2000**, *33*, 565.
(15) Howe, R. F.; Gratzel, M. *J. Phys. Chem.* **1985**, *89*, 4495.
(16) Howe, R. F.; Gratzel, M. *J. Phys. Chem.* **1987**, *91*, 3906.
(17) Micic, O. I.; Zhang, Y.; Cromack, K. R.; Trifunac, A. D.; Thurnauer, M. C. *J. Phys. Chem.* **1993**, *97*, 7277 and 13284.
(18) Micic, O. I.; Zhang, Y.; Cromack, K. R.; Trifunac, A. D.; Thurnauer, M. C. *J. Phys. Chem.* **1993**, *97*, 13284.
(19) Anpo, M.; Shima, T.; Fujii, T.; Suzuki, S.; Che, M. *Chem. Lett.* **1987**, 1997.
(20) Rajh, T.; Chen, L. X.; Lukas, K.; Liu, T.; Thurnauer, M. C.; Tiede, D. M. *J. Phys. Chem. B* **2002**, *106*, 10543.
(21) Weng, Y.-X.; Li, L.; Liu, Y.; Wang, L.; Yang, G.-Z. *J. Phys. Chem. B* **2003**, *107*, 4356.
(22) Rajh, T.; Nedeljkovic, J. M.; Chen, L. X.; Poluetkov, O.; Thurnauer, M. C. *J. Phys. Chem. B* **1999**, *103*, 3515.
(23) Kerssen, J.; Volger, J. *Physica (Utrecht)* **1973**, *69*, 535.
(24) Gilbert, B. C.; Lindsay Smith, J. R.; Taylor, P.; Ward, S.; Whitwood, A. C. *J. Chem. Soc., Perkin Trans. 2* **2000**, 2001.
(25) Guyard, L.; Hapiot, P.; Jouini, M.; Lacroix, J.-C.; Lagrost, C.; Neta, P. *J. Phys. Chem. A* **1999**, *103*, 4009.
(26) Godinez, L. A.; Swartz, L.; Criss, C. M.; Kaifer, A. E. *J. Phys. Chem. B* **1997**, *101*, 3376.
(27) Liu, J.; Ong, W.; Roman, E.; Lynn, M. J.; Kaifer, A. E. *Langmuir* **2000**, *16*, 3000.
(28) Recupero, F.; Bravo, A.; Bjorsvik, H.-R.; Fontana, F.; Minisci, F.; Piredda, M. *J. Chem. Soc., Perkin Trans. 2* **1997**, 2399.
(29) Hendrickson, D. N.; Sohn, Y. S.; Gray, H. B. *Inorg. Chem.* **1971**, *10*, 1550.
(30) Prins, R. *Mol. Phys.* **1970**, *19*, 603.
(31) Duggan, D. M.; Hendrickson, D. N. *Inorg. Chem.* **1975**, *14*, 955.
(32) Dong, T. Y.; Hwang, M. Y.; Lee, T. Y.; Tseng, L. H.; Peng, S. M., Lee, G. H. *J. Organomet. Chem.* **1991**, *414*, 227.
(33) Raybov, A. D.; Tyapochkin, E. M.; Varfolomeev, S. D.; Karyakin, A. A. *Bioelectrochem. Bioenerg.* **1990**, *24*, 257.
(34) Hirai, M.; Iwase, H.; Hayakawa, T.; Miura, K.; Inoue, K. *J. Synchrotron Rad.* **2002**, *9*, 202.
(35) Fischetti, R. F.; Rodi, D. J.; Mirza, A.; Irving, T. C.; Kondrashkina, E.; Makowski, L. *J. Synchrotron Rad.* **2003**, *10*, 398.
(36) Williamson, J. C.; Cao, J.; Ihee, H.; Frey, H.; Zewail, A. H. *Nature* **1997**, *386*, 159.
(37) Ihee, H.; Goodson, B. M.; Srinivasan, R.; Lobastov, V. A.; Zewail, A. H. *J. Phys. Chem. A* **2002**, *106*, 4087.
(38) Ihee, H.; Lobastov, V. A.; Gomez, U. M.; Goodson, B. M.; Srinivasan, R.; Ruan, C.-Y.; Zewail, A. H. *Science* **2001**, *292*, 458.
(39) Cao, J.; Ihee, H.; Zewail, A. H. *Proc. Natl. Acad. Sci. U.S.A.* **1999**, *96*, 338.
(40) Dudek, R. C.; Weber, P. M. *J. Phys. Chem. A* **2001**, *105*, 4167.
(41) Popovich, N. D.; Wong, S.-S.; Yen, B. K. H.; Yeom, H.-Y.; Paine, D. C. *Anal. Chem.* **2002**, *74*, 3127.
(42) Matsue, T.; Evans, D. H.; Osa, T.; Kobayashi, N. *J. Am. Chem. Soc.* **1985**, *107*, 3411.
(43) Chmurski, K.; Temeriusz, A.; Bilewicz, *Anal. Chem.* **2003**, *75*, 5687.